Biophysical Journal
Biophysical Letter

Asymmetric Phosphatidylethanolamine Distribution Controls Fusion Pore Lifetime and Probability

Alex J. B. Kreutzberger,[1] Volker Kiessling,[1] Binyong Liang,[1] Sung-Tae Yang,[1] J. David Castle,[2] and Lukas K. Tamm[1,*]

[1]Department of Molecular Physiology and Biological Physics and [2]Department of Cell Biology, Center for Cell and Membrane Physiology at the University of Virginia, Charlottesville, Virginia

ABSTRACT Little attention has been given to how the asymmetric lipid distribution of the plasma membrane might facilitate fusion pore formation during exocytosis. Phosphatidylethanolamine (PE), a cone-shaped phospholipid, is predominantly located in the inner leaflet of the plasma membrane and has been proposed to promote membrane deformation and stabilize fusion pores during exocytotic events. To explore this possibility, we modeled exocytosis using plasma membrane SNARE-containing planar-supported bilayers and purified neuroendocrine dense core vesicles (DCVs) as fusion partners, and we examined how different PE distributions between the two leaflets of the supported bilayers affected SNARE-mediated fusion. Using total internal reflection fluorescence microscopy, the fusion of single DCVs with the planar-supported bilayer was monitored by observing DCV-associated neuropeptide Y tagged with a fluorescent protein. The time-dependent line shape of the fluorescent signal enables detection of DCV docking, fusion-pore opening, and vesicle collapse into the planar membrane. Four different distributions of PE in the planar bilayer mimicking the plasma membrane were examined: exclusively in the leaflet facing the DCVs; exclusively in the opposite leaflet; equally distributed in both leaflets; and absent from both leaflets. With PE in the leaflet facing the DCVs, overall fusion was most efficient and the extended fusion pore lifetime (0.7 s) enabled notable detection of content release preceding vesicle collapse. All other PE distributions decreased fusion efficiency, altered pore lifetime, and reduced content release. With PE exclusively in the opposite leaflet, resolution of pore opening and content release was lost.

Membrane fusion is a necessary biological process for exocytosis, membrane trafficking, viral infection, and fertilization (1). Intracellular fusion as exemplified by exocytosis is mediated by a complex molecular machinery associated with the fusing membranes (2). At the core of this machinery are the soluble NSF attachment protein receptor (SNARE) proteins that alone are able to catalyze membrane fusion in vitro. According to current models, SNARE-mediated fusion occurs by formation of a stalk between the interacting membranes that elongates laterally and then opens to form a fusion pore that expands as the membranes fully fuse (3). Because highly curved membrane structures are necessary for the fusion pore and its preceding intermediates (4–7), lipid components that are favorable for generating curvature can enhance fusion (8). Phosphatidylethanolamine (PE) lipids are enriched in the inner leaflet of the plasma membrane (9,10); their conical shape confers a negative intrinsic curvature, which in turn could promote and stabilize pores during membrane fusion (11). It is therefore reasonable to hypothesize that the asymmetric distribution of PE between the two leaflets of the plasma membrane promotes fusion-pore formation in SNARE-mediated exocytosis and in models of this process. Simulations have predicted that PE could enhance the fusion rate when distributed on the outward facing leaflet of liposomes (12) or planar membranes (13). However, a comparative study of contrasting interleaflet PE distributions has not been performed due to the difficulty in preparing lipid bilayers with asymmetric lipid composition.

Recently, we reported SNARE-dependent fusion of purified dense core vesicles (DCVs; secretory vesicles from PC12 cells, an immortalized chromaffin cell line) with planar-supported bilayers containing the plasma membrane SNARE proteins syntaxin-1a and SNAP-25 (14). The supported bilayers were prepared by a two-step method that results in different lipid compositions of the first (substrate-proximal) and second (substrate-distal) leaflets (15–17). The DCVs contained neuropeptide Y (NPY) tagged with the fluorescent protein Ruby as content marker.

Submitted July 21, 2017, and accepted for publication September 13, 2017.

*Correspondence: lkt2e@virginia.edu

Alex J. B. Kreutzberger and Volker Kiessling contributed equally to this work.

Editor: Tobias Baumgart.

https://doi.org/10.1016/j.bpj.2017.09.014

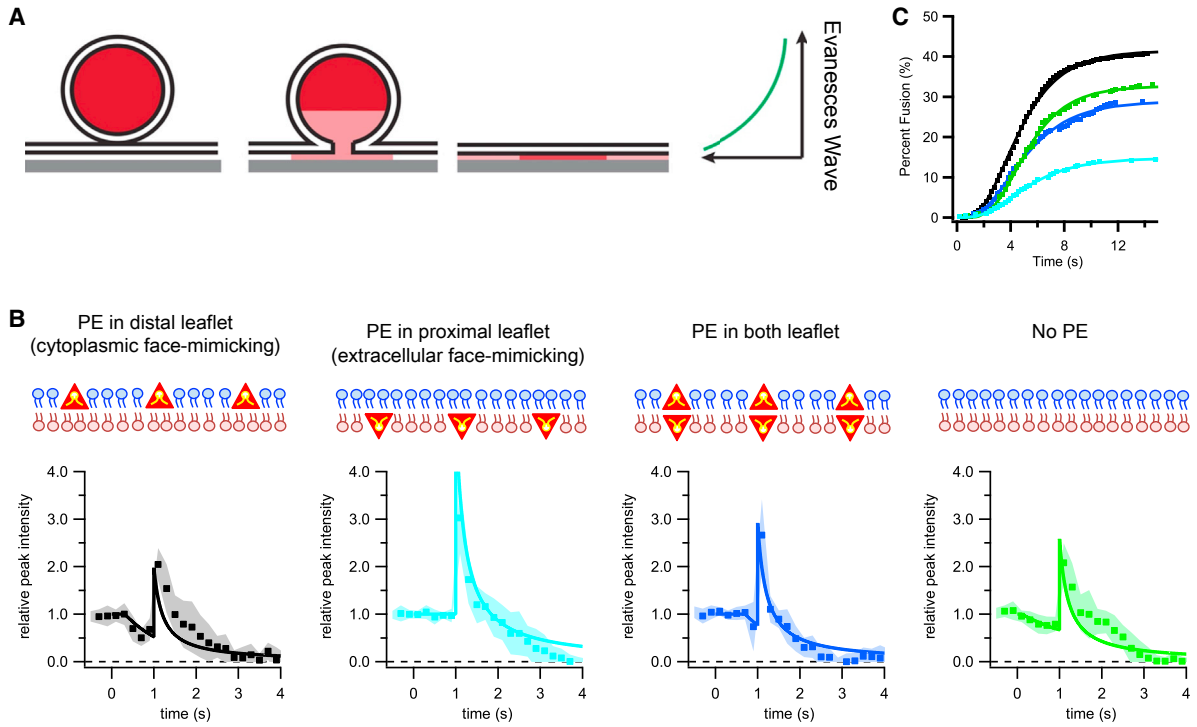

FIGURE 1 (*A*) Given here is a two-step model of DCV fusion event in a TIRF field. A DCV docks to a plasma membrane SNARE-containing planar-supported bilayer, where a fusion pore opens releasing the fluorescent NPY-Ruby from the DCV. The DCV then collapses into the supported bilayer, pulling NPY-Ruby forward in the TIRF field, which causes an increase in fluorescence as observed in the characteristic intensity traces of DCV fusion events. (*B*) Given here are characteristic fusion intensity traces for different distributions of PE in the supported bilayers. Dots are normalized intensities from 10 averaged fusion events, with SEs shown in shaded areas. Solid lines are fits of the two-step diffusion model shown in (*A*) with pore lifetimes of 0.7, 0, 0.3, and 1.5 s for PE in the distal, proximal, or both leaflets, or not present at all, respectively. A cartoon schematic of PE localization (*red triangles*) is shown above each figure, with blue and brown lipids representing the distal and proximal leaflets. (*C*) The kinetics of fusion are shown as cumulative distribution functions of the delay time between DCV docking and pore opening for PE in the distal leaflet (*black*), PE in the proximal leaflet (*cyan*), PE in both leaflets (*blue*), and no PE present (*green*).

Docking and fusion of single DCVs with the planar membrane was observed on a total internal reflection fluorescence (TIRF) microscope by following the fluorescence from NPY-Ruby. Upon docking, a sudden increase of fluorescence was detected as the DCV gets immobilized in the evanescent field. After a variable delay time, a first characteristic decay of fluorescent intensity occurs, followed by a sudden increase in fluorescence intensity, and ultimately a second characteristic decay of fluorescence was observed. This pattern is consistent with a two-step fusion process during which, first, a fusion pore opens, stays open whereas the DCV remains intact, and, in the second step, the DCV collapses into the planar membrane (Fig. 1 *A*). Fluorescent decays indicate diffusion of NPY-Ruby away from the fusion site and the intensity peak indicates a translocation of fluorescent content toward the substrate. A mathematical model that takes into account the characteristics of the evanescent electric field, the release rate through the fusion pore, and the lateral diffusion of NPY-Ruby within the cleft between the glass support and membrane, was able to reproduce the recorded fluorescence signal (14). In this model, the topology of the DCV was assumed not to change during the initial content release through the pore and NPY-mRuby in the DCV does not equilibrate, i.e., content is released first from within the proximity of the pore and only later from regions further away from the pore. A second requirement is that the lateral diffusion of NPY-mRuby away from the fusion site is faster during the first phase of release than after DCV collapse into the planar membrane. These conditions point to a relatively rigid luminal structure of the DCV protein content, which is strikingly similar to what was deduced from analyzing amperometric foot-signals measured during exocytotic events in chromaffin cells (18).

In this work we studied the effects of different PE distributions among the leaflets on fusion-pore stability, fusion efficiency, and fusion kinetics. We prepared plasma membrane SNARE-containing planar-supported bilayers under conditions with four different distributions of PE in the two leaflets: 1) 25 mol % in the distal leaflet facing the DCVs; 2) 25 mol % in the proximal (opposite) leaflet; 3) 25 mol % in both leaflets; and 4) no PE in either leaflet (Fig. 1 *B*). Condition 1 mimics the biological PE asymmetry of the plasma membrane and constitutes the same lipid distribution that was used in a recently published study (14).

The plasma membrane SNARE concentrations and orientations were the same under all four conditions (Fig. S2).

For each condition, we recorded at least 340 docking events of DCVs to plasma membrane SNARE-containing supported bilayers and evaluated their fusion efficiencies, fusion kinetics, and average line shapes, as described in detail in Kreutzberger et al. (14). The average line shapes measured under the different conditions were distinct in rate and length of the first decay as well as the following peak intensity (Fig. 1 *B*). The cumulative distribution functions of the time delays of the onset of fusion after docking were also different in the four cases (Fig. 1 *C*). The highest fusion efficiency, 41%, was achieved with PE in the distal, cytoplasmic face-mimicking leaflet of the target membrane. The fusion kinetics followed the same sigmoidal shape of previously reported single proteoliposome fusion events (Fig. 1 *C*; Table S1) (19). The fit of the fusion model to the average line shape of the fluorescence signal under condition 1 revealed a fusion pore that was open for 0.7 s and through which content was released with a characteristic rate of $(0.7\ s)^{-1}$ (Fig. 1 *B*; *black*). The diffusion coefficients for NPY-Ruby dispersion from the fusion site were 5 $\mu m^2/s$ during the initial release phase and 0.05 $\mu m^2/s$ after DCV collapse. These parameters are identical to the ones previously deduced under the same conditions (14), as recapitulated in the Supporting Material. For modeling the line shape of conditions 2–4, it was not necessary to change the two diffusion coefficients, showing that these parameters are independent of the fusion process.

For condition 2 (PE exclusively in the extracellular face-mimicking leaflet), fusion was strongly inhibited, with only ~15% of the docked DCVs undergoing fusion (Fig. 1 *C*, *cyan*). Moreover, the average line shape of these fusion events showed only a single phase, the collapse phase (Fig. 1 *B*, *cyan*). Within the time resolution of the measurement, 200 ms, no content release through a pore was detected and there was a compensatory increase in the fluorescence peak observed during DCV collapse. For condition 3 with symmetric PE distribution, the DCV fusion efficiency was 29%, about halfway between the two asymmetric conditions (Fig. 1 *C*, *blue*). Initial content release was observed and occurs at the same rate as under condition 1 $(0.7\ s)^{-1}$. However, the lifetime of the fusion pore was reduced to 0.3 s (Fig. 1 *B*, *blue*). For condition 4 (no PE; symmetric PC/cholesterol), the DCV fusion efficiency was 33% (similar to condition 3) (Fig. 1 *C*, *green*). In the average line shape, initial release of NPY-mRuby was clearly visible and the data were fitted with a characteristic release rate of $(1.5\ s)^{-1}$ and a fusion pore duration of 0.9 s (Fig. 1 *B*, *green*).

These results show that our hybrid system for reconstituting SNARE-mediated fusion in vitro using purified DCVs and supported membranes that contain only syntaxin-1a and SNAP-25 is able to reproduce the basic characteristics of single secretion events observed by amperometry of chromaffin cells (18). The fusion partners provide everything that is necessary to open a fusion pore and keep it open for almost 1 s. Our finding that the PE distribution is a key factor contributing to the presence of an initial release phase of NPY-Ruby through the stable fusion pore, has not been described before, to our knowledge. It experimentally confirms theories that invoke the importance of lipid shape in fusion intermediates. Indeed, under condition 1 with PE in the cytoplasmic-mimicking leaflet, about half of the fluorescent content is released before the DCV collapses into the planar target membrane. It is striking how well this asymmetric PE condition in our model membrane system not only promotes fusion with the highest efficiency but also reflects the electrophysiologically measured fusion events in cells (18). PE as a cone-shaped lipid most likely stabilizes the highly-curved local structure within the bilayer at the pore. Consistent with this view are our observations that no pore was observed when PE was present exclusively in the opposing leaflet and that a pore with shorter lifetime was observed with symmetrically distributed PE. Interestingly, when PE was absent on either side of the bilayer, release was observed over a longer time (0.9 s), but at a significantly slower rate. One interpretation of this result is that in the absence of PE, the pores transiently open and close instead of being stabilized by PE. This explanation is similar to that offered for single vesicle fusion as observed by TIRF microscopy by Stratton et al. (20).

In summary, we have shown how PE distribution contributes to the characteristic fluorescence profile that we observed in reconstituted SNARE-mediated fusion and how this distribution affects fusion probability, fusion pore stability, and the kinetics of DCV content release. In the future, our hybrid system should permit investigations of how other factors in the vesicle or plasma membrane influence the structure and stability of the exocytotic fusion pore.

SUPPORTING MATERIAL

Supporting Materials and Methods, Supporting Results, two figures, and one table are available at http://www.biophysj.org/biophysj/supplemental/S0006-3495(17)31026-3.

AUTHOR CONTRIBUTIONS

All authors designed the research, analyzed the data, and wrote or edited the article. A.J.B.K. and V.K. performed the research.

ACKNOWLEDGMENTS

We thank P. Kasson, D. Cafiso, and C. Stroupe for helpful discussions.

This work is supported by grant No. P01GM72694 from the National Institutes of Health (NIH).

SUPPORTING CITATIONS

References (21–34) appear in the Supporting Material.

REFERENCES

1. Martens, S., and H. T. McMahon. 2008. Mechanisms of membrane fusion: disparate players and common principles. *Nat. Rev. Mol. Cell Biol.* 9:543–556.
2. Südhof, T. C. 2013. Neurotransmitter release: the last millisecond in the life of a synaptic vesicle. *Neuron.* 80:675–690.
3. Hui, S. W., T. P. Stewart, …, P. L. Yeagle. 1981. Membrane fusion through point defects in bilayers. *Science.* 212:921–923.
4. Chizmadzhev, Y. A., F. S. Cohen, …, J. Zimmerberg. 1995. Membrane mechanics can account for fusion pore dilation in stages. *Biophys. J.* 69:2489–2500.
5. Chernomordik, L. V., and M. M. Kozlov. 2005. Membrane hemifusion: crossing a chasm in two leaps. *Cell.* 123:375–382.
6. Chernomordik, L. V., and M. M. Kozlov. 2008. Mechanics of membrane fusion. *Nat. Struct. Mol. Biol.* 15:675–683.
7. Jackson, M. B. 2009. Minimum membrane bending energies of fusion pores. *J. Membr. Biol.* 231:101–115.
8. Yeagle, P. L. 1989. Lipid regulation of cell membrane structure and function. *FASEB J.* 3:1833–1842.
9. Calderón, R. O., and G. H. DeVries. 1997. Lipid composition and phospholipid asymmetry of membranes from a Schwann cell line. *J. Neurosci. Res.* 49:372–380.
10. van Meer, G., D. R. Voelker, and G. W. Feigenson. 2008. Membrane lipids: where they are and how they behave. *Nat. Rev. Mol. Cell Biol.* 9:112–124.
11. Churchward, M. A., T. Rogasevskaia, …, J. R. Coorssen. 2008. Specific lipids supply critical negative spontaneous curvature—an essential component of native Ca^{2+}-triggered membrane fusion. *Biophys. J.* 94:3976–3986.
12. Kasson, P. M., and V. S. Pande. 2007. Control of membrane fusion mechanism by lipid composition: predictions from ensemble molecular dynamics. *PLOS Comput. Biol.* 3:e220.
13. Risselada, H. J. 2017. Membrane fusion stalks and lipid rafts: a love hate relationship. *Biophys. J.* 112:2475–2478.
14. Kreutzberger, A. J. B., V. Kiessling, …, L. K. Tamm. 2017. Reconstitution of calcium-mediated exocytosis of dense-core vesicles. *Sci. Adv.* 3:e1603208.
15. Kalb, E., S. Frey, and L. K. Tamm. 1992. Formation of supported planar bilayers by fusion of vesicles to supported phospholipid monolayers. *Biochim. Biophys. Acta.* 1103:307–316.
16. Crane, J. M., V. Kiessling, and L. K. Tamm. 2005. Measuring lipid asymmetry in planar supported bilayers by fluorescence interference contrast microscopy. *Langmuir.* 21:1377–1388.
17. Kiessling, V., B. Liang, and L. K. Tamm. 2015. Reconstituting SNARE-mediated membrane fusion at the single liposome level. *Methods Cell Biol.* 128:339–363.
18. Albillos, A., G. Dernick, …, M. Lindau. 1997. The exocytotic event in chromaffin cells revealed by patch amperometry. *Nature.* 389: 509–512.
19. Domanska, M. K., V. Kiessling, and L. K. Tamm. 2010. Docking and fast fusion of synaptobrevin vesicles depends on the lipid compositions of the vesicle and the acceptor SNARE complex-containing target membrane. *Biophys. J.* 99:2936–2946.
20. Stratton, B. S., J. M. Warner, …, B. O'Shaughnessy. 2016. Cholesterol increases the openness of SNARE-mediated flickering fusion pores. *Biophys. J.* 110:1538–1550.
21. Pabst, S., J. W. Hazzard, …, D. Fasshauer. 2000. Selective interaction of complexin with the neuronal SNARE complex. Determination of the binding regions. *J. Biol. Chem.* 275:19808–19818.
22. Liang, B., V. Kiessling, and L. K. Tamm. 2013. Prefusion structure of syntaxin-1A suggests pathway for folding into neuronal trans-SNARE complex fusion intermediate. *Proc. Natl. Acad. Sci. USA.* 110:19384–19389.
23. Dawidowski, D., and D. S. Cafiso. 2013. Allosteric control of syntaxin 1a by Munc18-1: characterization of the open and closed conformations of syntaxin. *Biophys. J.* 104:1585–1594.
24. Kreutzberger, A. J., B. Liang, …, L. K. Tamm. 2016. Assembly and comparison of plasma membrane SNARE acceptor complexes. *Biophys. J.* 110:2147–2150.
25. Domanska, M. K., V. Kiessling, …, L. K. Tamm. 2009. Single vesicle millisecond fusion kinetics reveals number of SNARE complexes optimal for fast SNARE-mediated membrane fusion. *J. Biol. Chem.* 284:32158–32166.
26. Wagner, M. L., and L. K. Tamm. 2001. Reconstituted syntaxin1a/SNAP25 interacts with negatively charged lipids as measured by lateral diffusion in planar supported bilayers. *Biophys. J.* 81:266–275.
27. van den Hoff, M. J., A. F. Moorman, and W. H. Lamers. 1992. Electroporation in 'intracellular' buffer increases cell survival. *Nucleic Acids Res.* 20:2902.
28. Kiessling, V., J. M. Crane, and L. K. Tamm. 2006. Transbilayer effects of raft-like lipid domains in asymmetric planar bilayers measured by single molecule tracking. *Biophys. J.* 91:3313–3326.
29. Zhang, Z., Y. Wu, …, M. B. Jackson. 2011. Release mode of large and small dense-core vesicles specified by different synaptotagmin isoforms in PC12 cells. *Mol. Biol. Cell.* 22:2324–2336.
30. Kiessling, V., and L. K. Tamm. 2003. Measuring distances in supported bilayers by fluorescence interference-contrast microscopy: polymer supports and SNARE proteins. *Biophys. J.* 84:408–418.
31. Zareh, S. K., M. C. DeSantis, …, Y. M. Wang. 2012. Single-image diffusion coefficient measurements of proteins in free solution. *Biophys. J.* 102:1685–1691.
32. Fromherz, P., V. Kiessling, …, G. Zeck. 1999. Membrane transistor with giant lipid vesicle touching a silicon chip. *Appl. Phys. A.* 69:571–576.
33. Kiessling, V., B. Müller, and P. Fromherz. 2000. Extracellular resistance in cell adhesion measured with a transistor probe. *Langmuir.* 16:3516–3521.
34. Press, W. H., B. P. Flannery, …, W. T. Vetterling. 1986. Numerical Recipes: The Art of Scientific Computing.. Cambridge University Press, Cambridge, United Kingdom.